Quasi-Fermi-Level Splitting of Cu-Poor and Cu-Rich CuInS$_2$ Absorber Layers

Alberto Lomuscio,[1,*] Tobias Rödel,[1] Torsten Schwarz,[2] Baptiste Gault,[2] Michele Melchiorre,[1] Dierk Raabe,[2] and Susanne Siebentritt[1]

[1]*Laboratory for Photovoltaics, Physics and Materials Science Research Unit, University of Luxembourg, 44, rue du Brill, 4422 Belvaux, Luxembourg*
[2]*Max-Planck-Institut für Eisenforschung, Max-Planck-Straße 1, 40237 Düsseldorf, Germany*

Cu(In, Ga)S$_2$-based solar cells are interesting tandem partners for Si or chalcopyrite solar cells, but suffer from a low open-circuit voltage. Recently, record efficiencies have been achieved by using higher growth temperatures for the absorber. To understand the effect of higher growth temperatures, we investigate the structural and electronic properties of CuInS$_2$ absorbers. By investigating the absorber alone as opposed to complete solar cells, we can separate changes in the absorber from effects of the interface properties. We show that the quasi-Fermi-level splitting, which indicates the maximum open-circuit voltage an absorber is capable of, increases with higher growth temperature. The quasi-Fermi-level splitting is limited by a deep defect, the concentration of which decreases with higher growth temperature and is less prominent in Cu-rich films. Thus, we demonstrate that the open-circuit voltage of CuInS$_2$-based solar cells is limited to below 850 mV by the absorber itself, independent of the interface. In contrast to the changes in the electronic properties, the structural properties are rather independent of temperature within the range investigated but are significantly influenced by the composition.

I. INTRODUCTION

Copper indium gallium disulfide, Cu(In, Ga)S$_2$, is a promising absorber material for thin-film solar cells due to its band-gap energy (E_g) that can be tuned between 1.55 (pure CIS) and 2.53 eV (pure CGS) [1]. This range matches the solar spectrum well [2] and makes Cu(In, Ga)S$_2$ suitable for both single [3] and tandem devices [4].

In the field of pure-sulfide Cu(In, Ga)S$_2$ single-junction cells, over the past decades, most of the record conversion efficiencies were achieved with absorber layers grown under Cu excess condition, i.e., $[Cu]/([Ga] + [In]) > 1$ (Cu rich), regardless of the deposition process [5–7].

The new breakthrough for this chalcopyrite material came when Hiroi and co-workers reached good electrical performances by growing absorbers under Cu deficiency (Cu poor) and using processing temperatures above those used traditionally ($>550\,°C$) [8]. They reached the world record efficiency of 15.5% on both potassium-cyanide- (KCN-) free and Cd-free pure sulfide Cu(In, Ga)S$_2$ solar

cells [9] and they achieved the highest open-circuit voltage V_{OC} of 973 mV [10]. Recently, the same group has announced a new (unconfirmed) record, 16.9%, of pure-sulfide-based solar cells, by optimizing the interface between the back contact and the absorber [11].

However, Cu(In, Ga)S$_2$-based solar cells still suffer from a low efficiency compared to their counterpart Cu(In, Ga)Se$_2$-based solar cells, which have reached an efficiency of 23.35% [12]. This is mainly due to a low open-circuit voltage with respect to the band gap in the sulfide solar cells. In fact, the champion sulfide-based device has a V_{OC} of 920 mV [9], that represents a V_{OC} loss defined as $E_g/q - V_{OC}$ of approximately 630 mV with q elementary charge, whereas for selenide-based solar cells the V_{OC} loss is only about 400 mV [13]. Many parameters can influence the V_{OC} of a solar cell, such as recombinations in the bulk of the absorber, at the back contact or at the interface between the absorber and the buffer layer. This last issue is highly relevant in pure-sulfide cells, because of the unsuitable band alignment between the absorber and the common cadmium sulfide (CdS) layer used as the buffer layer [14,15]. Much effort has been devoted to optimizing the buffer layer, replacing the CdS with wider band-gap materials, like zinc oxysulfide [Zn(S, O)], but without significant improvement in V_{OC} [16,17].

Quasi-Fermi-level splitting (QFLS) is a mark of the recombination activity of the absorber itself, and it

---

*alberto.lomuscio@uni.lu

represents an upper limit for the open-circuit voltage. Furthermore, it can be measured by calibrated PL spectroscopy without making the whole device and thus without including the effects of unfavorable band alignment at the front interface [18,19].

Since it was shown that higher growth temperatures improve the device efficiency, we investigate here the role of the growth temperature on the quality of the absorbers prepared using a wide range of deposition parameters. We report results from calibrated PL measurements performed at room temperature on bare $CuInS_2$ to reveal the effect of deposition temperature on QFLS. We limit ourselves to the pure In compound to avoid phase segregation if Ga is added [20]. Furthermore, $CuInS_2$ absorbers have a simpler structure than those based on $Cu(In, Ga)S_2$, as alloying with Ga increases the band gap and would lead to bandgap grading [8]. We show that, on the one hand, a higher deposition temperature does not influence significantly the morphology or structural properties of the films, as confirmed by XRD and TEM analysis; on the other hand, it dramatically increases the QFLS of the corresponding CIS absorbers, regardless of composition. Moreover, we show that using higher processing temperatures, the intensity of a broad deep-defect band in PL drastically decreases. Thus, we conclude that the main effect of an increased growth temperature is to reduce the density of a specific deep defect, which is responsible for nonradiative recombination, leading to higher QFLS.

II. EXPERIMENTAL DETAILS

$CuInS_2$ (CIS) absorbers are deposited on Mo-coated soda lime glass (SLG) by co-evaporation of Cu, In, and S in a physical vapor-deposition system. The samples grown under Cu excess are prepared both in a one-stage co-evaporation process with constant fluxes throughout the deposition duration at two different substrate temperatures (550 °C and 590 °C) and in a two-stage process, with a In and S deposition at 250 °C followed by a Cu and S deposition at 550 or 590 °C. The secondary phase CuS_x for the Cu-rich samples is removed by KCN etching performed with a 10% aqueous solution for 5 min. After this cyanide treatment, the Cu : In ratio is close to 1, determined by energy dispersive x-ray (EDX) spectroscopy. The Cu-poor absorbers are deposited in a one-stage co-evaporation process, both at 550 and 600 °C.

Some of the CIS absorbers are made into solar cells with a CdS or $Zn(S, O)$ buffer layer deposited by chemical bath deposition, sputtered intrinsic ZnO and ZnO:Al window layers and finally e-beam deposited Ni/Al contact grids.

The PL measurements are carried out in a home-built system with a 660-nm wavelength laser as the excitation source. The emitted luminescence is collected by two off-axis mirrors, focused into a fiber, spectrally resolved by a monochromator and detected by a Si-CCD and an (In,Ga)As-CCD array. For intensity calibration and thus for the determination of the QFLS, two corrections are applied to the raw data. The spectral correction is performed using a commercial calibration lamp with a known spectrum. For the intensity calibration, the beam diameter is measured with a CCD camera and the laser power with a power meter. With this, the incident photon flux is calculated and related to the photon flux of the AM 1.5 sun spectrum above the band gap. The calibrated luminescence spectra are converted to energy dependence and evaluated by means of Planck's generalized law, which describes the PL yield depending on the energy as a function of absorptivity, temperature, and the QFLS [18]. By fitting the high-energy slope at photon energies sufficiently larger than the band gap, the absorptivity can be assumed unity and, thus, the QFLS is extracted [18]. The temperature used for the fitting is measured by a pyrometer. For further details see the Supplemental Material of [21]. It has been demonstrated that optical corrections lead only to small changes of the QFLS values, while they are fundamental to get reliable absorption coefficient values [22].

For measurements at 80 K, the samples are introduced into a liquid-helium flow cryostat and are measured by the same optical setup.

Current-voltage characteristics (*J-V*) are measured with an AAA solar simulator under the equivalent illumination of an AM 1.5 spectrum.

The structural properties of the absorber layers are studied by XRD, SEM, and STEM.

III. RESULTS AND DISCUSSION

We investigate the effect of deposition temperature on the properties of $CuInS_2$ thin films prepared using a wide range of deposition parameters. Concerning those grown under Cu excess, we use both the one-stage and two-stage processes: in the former case, both the elemental fluxes and substrate temperature are kept constant, while, for the latter, a deposition of In and S at low temperature is followed by a Cu and S deposition at higher temperature. For samples deposited under Cu deficiency, only the one-stage process is used. More details are reported in Table I. The Cu:In values for the Cu-rich samples are referred to as the ratios before KCN etching, performed to remove the CuS_x secondary phase(s) [23].

TABLE I. Summary of the samples studied.

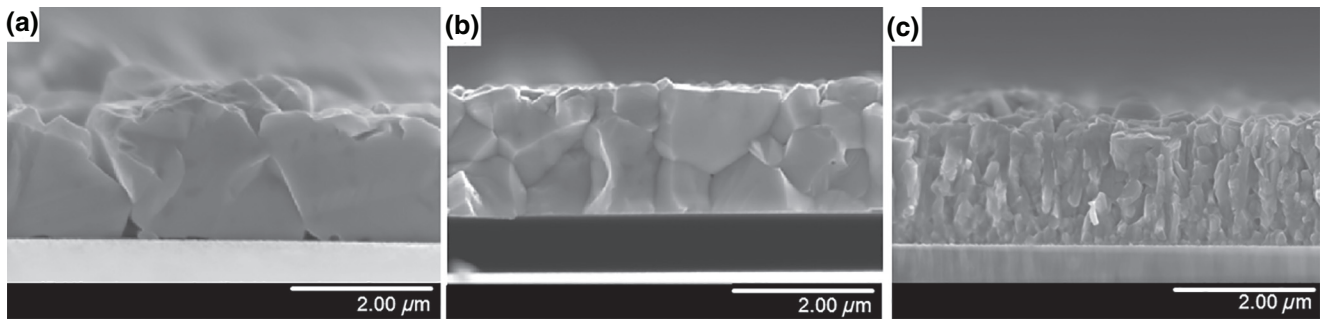|	Cu:In	Process	T_{dep} (°C)
Sample A	1.8	One-stage	550
Sample B	1.8	One-stage	590
Sample C	1.5	Two-stage	$250 + 550$
Sample D	1.5	Two-stage	$250 + 590$
Sample E	0.9	One-stage	550
Sample F	0.9	One-stage	600

FIG. 1.   SEM cross sections showing the morphology of the $CuInS_2$ layers grown at $550\,°C$ by (a) Cu-rich one-stage, (b) Cu-rich two-stage, and (c) Cu-poor one-stage processes.

A. Effect of temperature on (micro) structural properties

Before discussing the effects of deposition temperature (T_{dep}), we show the effect of stoichiometry and process configuration (single- and multistage process) on morphology and microstructural properties for co-evaporated absorbers in Figs. 1 and 2, respectively.

Figure 1 shows SEM cross sections of $CuInS_2$ absorber layers, deposited at $550\,°C$ under Cu excess following the one-stage and two-stage process [Figs. 1(a) and 1(b), respectively] and under Cu deficiency [Fig. 1(c)]. These micrographs are obtained after etching the CuS_x secondary phase, which is present in as-grown Cu-rich films [23]. For both Cu-rich films, the grain size is in the micrometer range, while the Cu-poor samples have a much smaller grain size. However, in Fig. 1(a), we can clearly see the presence of deep trenches between the grains, voids, and poor adhesion on the back side of the film and a rough surface. In contrast, the two-stage Cu-rich film shows a denser layer with a smoother surface. The features of the Cu-rich layers can be attributed to the segregation of the secondary phase CuS_x, which only occurs during the last stage of the film growth in the two-stage process [24]. In contrast, CuS_x

is formed throughout the duration of the one-stage process and can form grains that extend far into the film. After the etching, these grains leave the deep trenches behind. These morphological features have a strong influence on the final device performances, as we discuss in the following.

The corresponding CIS absorber layers deposited using higher growth temperature do not show any significant difference in grain size and morphology, as shown in Fig. S1 within the Supplemental Material [31].

The analysis performed by TEM on Cu-poor and Cu-rich one-stage samples reveals significant differences in microstructure, as well. Figure 2 displays cross-section scanning TEM images of $Mo/CuInS_2/CdS$ stacked layers: the Cu-poor sample [Fig. 2(a)] is characterized by a dense network of defects such as dislocations and stacking faults as well as by small-sized grains, whereas the Cu-rich sample reveals a drastic reduction in defect density [Fig. 2(b)]. A common feature for both thin films is the presence of smaller grains at the interface between the Mo back contact and the absorber. Figures 2(c) and 2(d) report the STEM images of the corresponding films grown at higher temperature. They do not show a drastic change in microstructure with increasing temperature.
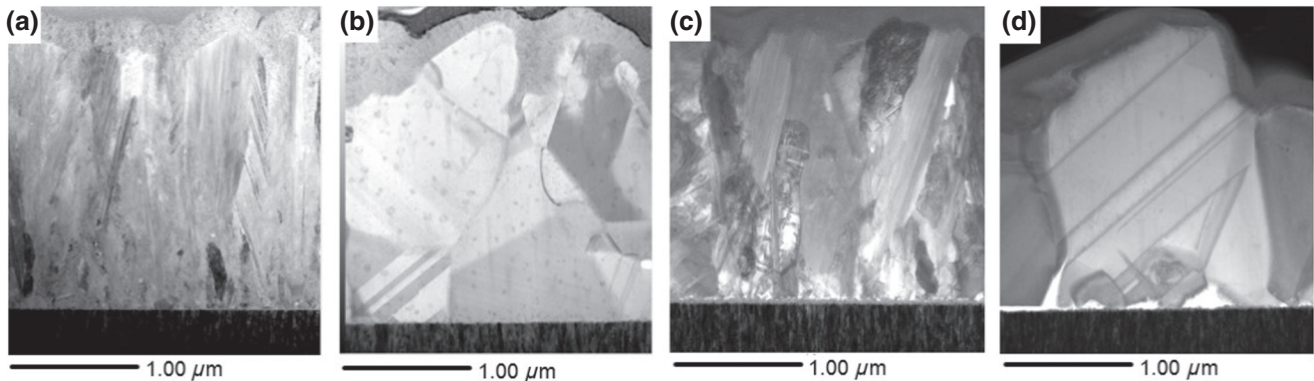

FIG. 2.   STEM cross section images showing the microstructure of the $CuInS_2$ absorber layers grown in one-stage configuration: Cu poor deposited at (a) 550 and (c) $600\,°C$, and Cu rich deposited at (b) 550 and (d) $590\,°C$.
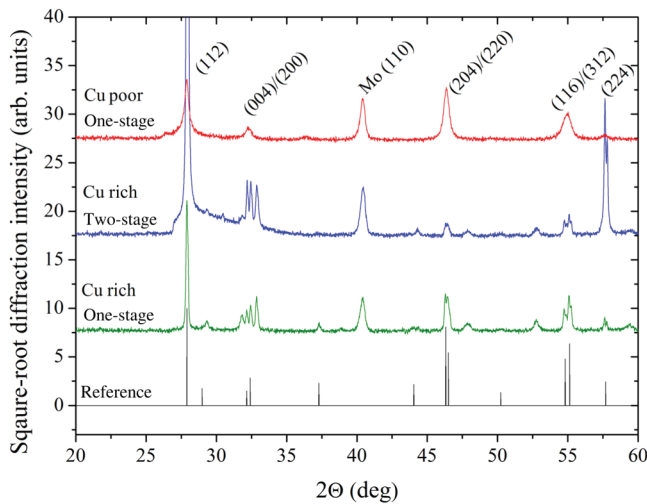
FIG. 3.   XRD patterns of CIS layers deposited at 550 °C; the reference CIS (ICDD PDF 00-047-1372) is in black.

Figure 3 illustrates the XRD patterns of the layers shown in Fig. 1, but before removing the CuS secondary phase by KCN etching of the Cu-rich samples.

The Θ–2Θ patterns reveal that the texture of CuInS$_2$ is sensitive to growth conditions: the films deposited under Cu deficiency have a (204)-(220) preferred orientation, according to powder diffraction data (ICDD PDF 00-047-1372). In contrast, the Cu-rich samples grown in the one-stage process show a close to (112) preferred orientation, which is even stronger for the Cu-rich film deposited by the two-stage process. Moreover, for both kinds of Cu-rich samples, the tetragonal splitting is seen for (004)/(200) and (116)-(312) diffraction lines: it is a characteristic sign of the tetragonal structure and an indicator of the crystalline quality of these films. No differences in the preferred orientation is found between films deposited at lower and higher temperature (Fig. S2 within the Supplemental Material [31]).

Thus we observe dramatic changes in the structural properties with the composition, but hardly any with the growth temperature within the range investigated.

B. Effect of temperature on the optoelectronic properties

The effect of T_{dep} on the recombination properties of the absorber layers studied in this work is analyzed by means of PL performed both at room and low temperatures (80 K). Figure 4(a) shows the room-temperature PL of Cu-rich samples deposited by the one-stage process after KCN etching. It should be noted that the PL intensity of uncovered CuInS$_2$ films does not degrade with time, in contrast to the behavior of selenide Cu(In, Ga)Se$_2$ films [21,25]. Both spectra show a band around 1.51 eV, which is related to band-band transitions and a broad
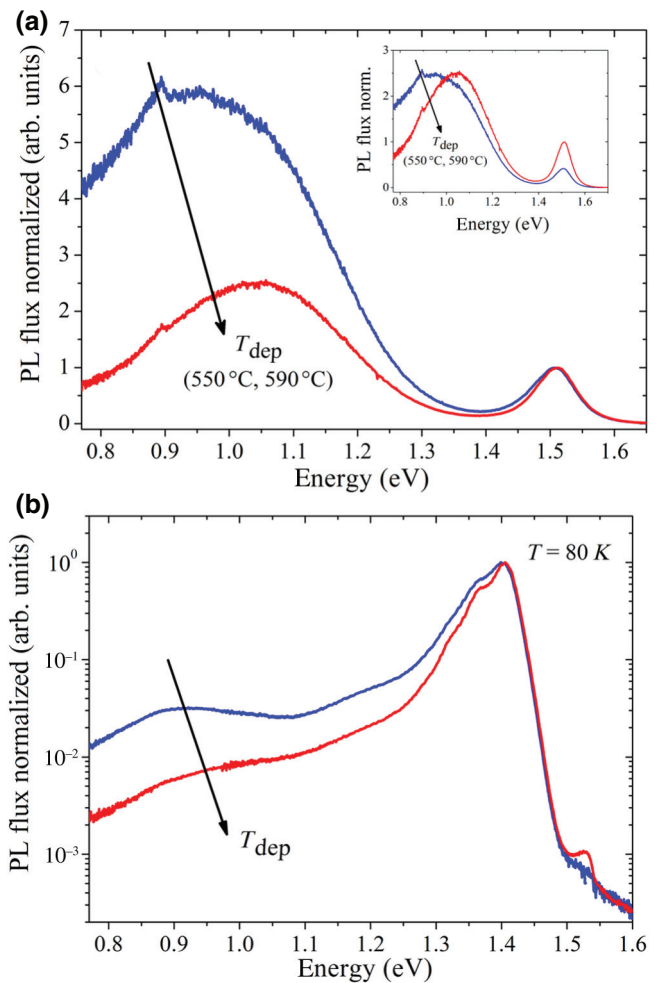

FIG. 4.   (a) Room- and (b) low-temperature (80 K) PL of Cu-rich one-stage samples deposited at 550 (blue) and 590 °C (red). The insert in (a) shows the same spectra normalized to the deep band. Note that results are displayed (a) in a linear scale and (b) in a log scale.

deeper band. The spectra are normalized to the band-band transition. It is observed that the relative intensity of the broad deeper band decreases when higher deposition temperatures are used (550 and 590 °C in the present case), indicating a better optoelectronic quality of this absorber with a lower concentration of deep defects. The corresponding two-stage Cu-rich samples grown at different T_{dep} show a similar trend in terms of the broad deep-band intensity (not shown here). Cu-poor absorbers, deposited at 550 °C do not even show the band-gap luminescence, but only the low-energy PL, whereas the Cu-poor sample deposited at high temperature (600 °C) has luminescence also at 1.5 eV. A comparison of the room-temperature PL spectra of the different samples deposited at high T_{dep} is reported in Fig. S3 within the Supplemental Material [31].

The inset in Fig. 4(a) demonstrates that the deep-defect luminescence also gets narrower, not only lower. This is

the first indication that there might actually be two transitions and the one at lower energies around 0.8–0.9 eV decreases more with higher growth temperatures.

The low-temperature PL carried out at 80 K [Fig. 4(b)] for the same samples as reported in Fig. 4(a) shows again the same trend: a lower contribution of deep-defect luminescence with higher growth temperature. Furthermore, it confirms that a deep-defect luminescence around 0.9 eV is present with an intensity that decreases with higher deposition temperatures.

Both films show luminescence peaks around 1.4 eV. These PL bands have been observed in the literature and have been attributed to shallow defects [26,27].

The PL spectra measured at 80 K indicate also that the film grown at higher temperature shows band-gap luminescence around 1.52 eV, related to the excitonic emission. The occurrence of band-gap luminescence indicates once more the higher optoelectronic quality of the film grown at higher temperature.

This interpretation is confirmed by the corresponding QFLS values measured at photon fluxes equivalent to 1 sun, shown in Fig. 5 for all films studied here. Both one-stage and two-stage Cu-rich samples deposited at 590 °C have higher QFLS than those grown at 550 °C: +33 and +37 meV, respectively. Concerning the Cu-poor samples deposited at lower T_{dep}, the PL signal is too low to analyze in terms of QFLS, indicating a very low QFLS; for the absorber deposited at 600 °C, a QFLS of 670 meV is found.

It is seen that beyond the temperature effect, the stoichiometry also influences the quality of the absorbers. In fact, comparing the one-stage samples grown under Cu deficiency and Cu excess, the average QFLS of the latter is higher. Concerning the Cu-rich samples deposited in
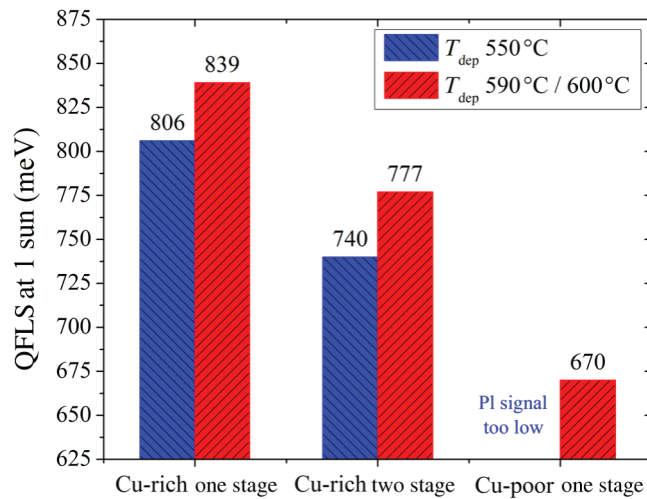
the one- or two-stage process, whether the lower QFLS of the latter is due to the different processes (thus to different structural properties) or due to the dissimilar Cu excess, cannot yet be clarified.

The observation of higher QFLS in Cu-rich $CuInS_2$ absorbers is in contrast to the observations on selenide chalcopyrites: although the Cu-rich selenide absorbers show a range of favorable properties [28], their QFLS is lower than that of their Cu-poor counterparts [21].

To summarize the observations from PL: the higher growth temperature leads to a reduction of the intensity of the PL band related to the deep defect, as well as to an increment in the quasi-Fermi-level. In order to establish the correlation between the QFLS values and the intensity of the broad deep band, the PL spectra of several Cu-rich one-stage samples are fitted with three different Gaussian bands, as shown in Fig. 6(a). The band around 1.5 eV is indisputably present and is due to the band-gap luminescence. Concerning the deep band: although at first sight it could be described by a single band, it is actually a convolution of two distinct bands: the one around 1.05 eV and the one around 0.8 eV. The PL band around 0.8 eV is justified because (i) the room-temperature broad deep PL band is asymmetric as seen in Fig. 6(a), (ii) the room-temperature deep-defect PL becomes narrower with increasing growth temperature, as seen in Fig. 4(a), (iii) the low-temperature PL in Fig. 4(b) shows that the band shape of the deep luminescence indicates the presence of a distinct band in this spectral region. For each of these bands we calculate the relative ratio of the integrated single-band intensity over the entire PL-spectra intensity ($r_i = I_i/\Sigma I_i$). The three different ratios are labeled, respectively, r_{BB}, $r_{1.05}$, $r_{0.8}$. Figure 6(b) reports the trend of these ratios with the QFLS of the samples. QFLS are measured at higher fluxes than 1 sun, to ease the measurement. The trend of r_{BB} with QFLS is evident: in an ideal absorber, we expect only radiative recombination and the PL spectrum should show only the band-to-band transition. Therefore, when r_{BB} increases, the quality of the absorber is improved, leading to higher QFLS. An unexpected trend is the one of $r_{1.05}$: the QFLS increases with an increasing share of this deep-defect luminescence. The reason becomes clear, when investigating the ratio $r_{0.8}$: it shows an opposite trend compared to $r_{1.05}$, and its drop leads to a higher QFLS value. This indicates that the QFLS is limited by the defects involved in the transition around 0.8 eV. With a lower contribution of deep defects around 0.8 eV, all other radiative transitions are increased, including the one at 1.05 eV.

Thus, the fewer deep defects involved in the transition around 1.05 eV does not limit QFLS. In fact, from the spectra normalized to the amplitude of the broad deep band shown in the insert in Fig. 4(a), the main difference using a higher growth temperature occurs for energies lower than 1 eV. Once the density of deep defects is reduced

FIG 5. QFLS at 1 sun measured for the samples investigated in this work. For high-T deposition, 590 °C is used for Cu-rich films, whereas 600 °C is used for one-stage Cu-poor films.
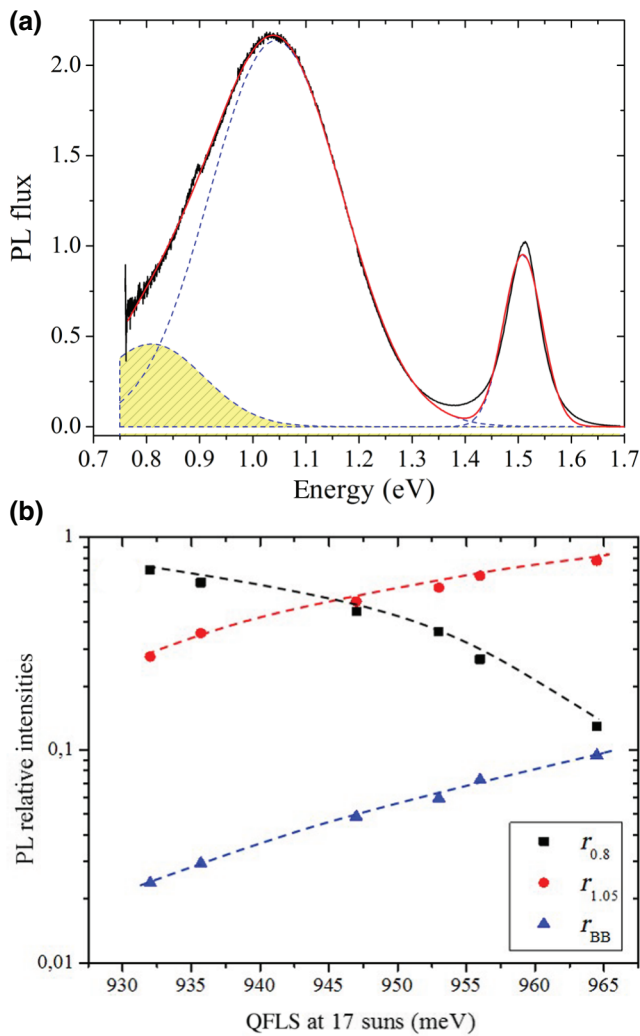
FIG 6. (a) Fitting of room-temperature PL spectrum: the deeper band centered at around 0.8 eV is highlighted in yellow. (b) PL relative intensities with the QFLS of the samples.
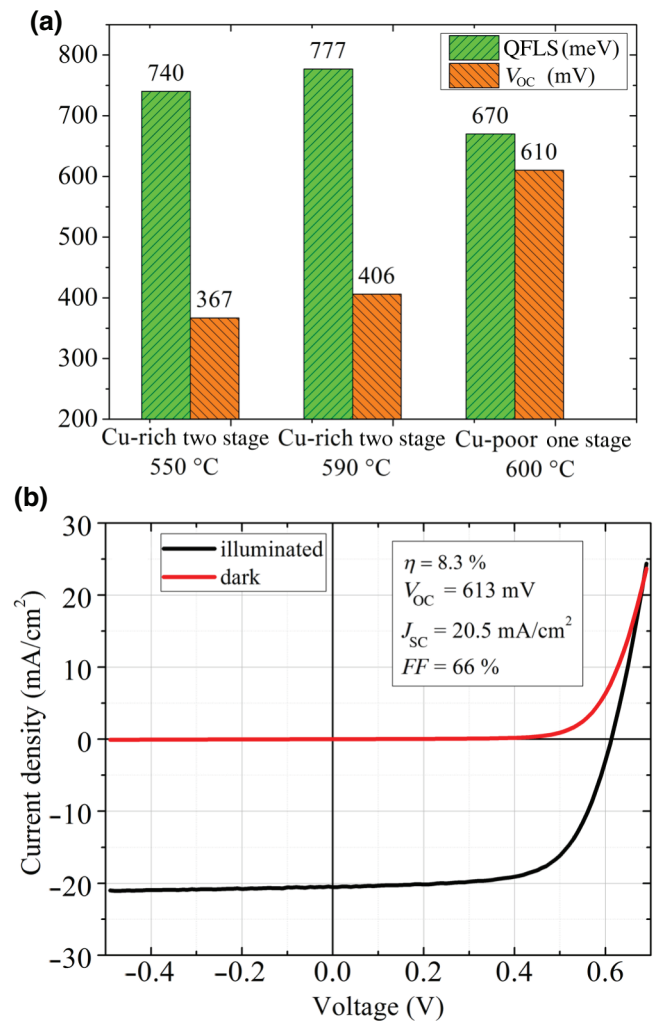

FIG. 7. (a) Comparison of the V_{OC} and QFLS of Cu-rich and Cu-poor absorbers; the gap for the Cu-rich samples can be drastically reduced, improving the buffer-layer interface; (b) *J-V* characteristic under AM1.5 illumination for the best cell of this work. Solar cells based on Cu-poor absorbers deposited at low temperature do not show any diode behavior.

sufficiently, it is expected that the QFLS might be limited by the defects of the 1.05-eV transition.

Solar cells are made with absorbers prepared by the same deposition run as the films discussed above (Table I and Fig. 5). Figure 7(a) shows the average open-circuit voltage V_{OC} of these devices together with the corresponding QFLS values. The solar cells based on one-stage Cu-rich films are not included, since their current-density–voltage (*J-V*) characteristics are dominated by a significant shunting behavior. This is attributed to the unfavorable morphology of these films, as seen in Fig. 1(a) and commonly reported in the literature [5,7]. The EDX mapping shown in Fig. S4(a) within the Supplemental Material indicates clearly that the CdS buffer extends deep into the absorber layer along the grain boundaries, down to the interface between Mo and the absorber layer. These features are expected to cause the low shunt resistance of the

Cu-rich cells made by the one-stage process and have to be avoided to achieve working solar cells.

For the devices based on two-stage Cu-rich absorbers deposited at low and high temperature, the increment with higher growth temperature in QFLS of 37 meV is reflected by the improvement in the V_{OC} of 39 mV. However, the Cu-rich cells, although exhibiting higher QFLS, show a considerably lower V_{OC} than the Cu-poor cells. The Cu-poor solar cells show an average V_{OC} value of 610 mV. The *J-V* characteristic under AM 1.5 illumination for the best cell of this work is reported in Fig. 7(b). It is based on a Cu-poor absorber grown by the one-stage process at 600 °C and has an efficiency η of 8.3%, with a short-circuit current $J_{SC} = 20.5$ mA/cm², $V_{OC} = 613$ mV, and fill factor FF = 66%. It should be noted, that these cells do not

contain Ga. Thus, this efficiency compares not unfavorably with the best efficiency reported for pure CuInS$_2$ of 12.2% [29].

The huge gap between the QFLS and the V_{OC} for the Cu-rich samples cannot be attributed to the absorber itself, but originates from a loss that occurs at the interfaces of the solar cell and is likely due to the buffer layer and/or the buffer-absorber interface. It is well known that Cu-rich chalcopyrite-based solar cells are dominated by interface recombination, in contrast to solar cells based on Cu-poor absorbers [30]. As discussed by Braunger *et al.* in Ref. [29], the preparation conditions of the chemical bath deposition of CdS can play a significant role in the final device performance. In fact, we use the same kind of absorber with a QFLS of 740 meV to fabricate solar cells with CdS using higher thiourea concentration during the deposition or with Zn(O, S) as the buffer layer. In both cases, a higher average value of V_{OC} is found with 480 and 600 mV, respectively. This improved V_{OC} is not due to a change in absorber quality, but due to a change in interface quality. This is a clear indication that many factors may affect V_{oc}, whereas the QFLS gives a direct indication of the quality of the absorber itself without the influence of interfaces and contact layers. Thus to improve the absorber itself, it is necessary to investigate QFLS.

IV. CONCLUSIONS

It has been observed in the past that higher deposition temperatures improve CuInS$_2$ solar cells [8]. Here, we show that the main effect of a higher deposition temperature is an improvement of the electronic structure by reducing the density of a deep defect. This deep defect is responsible for the PL band around 0.8 eV. It is this deep defect that is responsible for the limitation of quasi-Fermi-level splitting in CuInS$_2$ absorbers. Another deep defect that exhibits luminescence around 1.05 eV is not limiting QFLS in our absorbers, but will become critical as soon as the deeper defect is reduced sufficiently. Higher growth temperature reduces the concentration of both deep defects and thus increases the QFLS of the absorbers. Furthermore, for all growth temperatures Cu-rich absorbers have higher QFLS than Cu-poor ones. The higher QFLS of Cu-rich absorbers does not convert into a higher V_{OC}, because of an unfavorable interface with the buffer layer in this case. The improvement of the QFLS with higher growth temperature leads to a corresponding improvement of the V_{OC} of the completed cells.

[1] B. Tell, J. Shay, and H. Kasper, Electrical properties, optical properties, and band structure of CuGaS$_2$ and CuInS$_2$, Phys. Rev. B **4**, 2463 (1971).

[2] S. Siebentritt, What limits the efficiency of chalcopyrite solar cells?, Sol. Energy Mater. Sol. Cells **95**, 1471 (2011).

[3] T. Kirchartz and U. Rau, What makes a good solar cell?, Adv. Energy Mater **8**, 1703385 (2018).

[4] S. Siebentritt, High voltage, please!, Nat. Energy **2**, 840 (2017).

[5] R. Kaigawa, A. Neisser, R. Klenk, and M-Ch Lux-Steiner, Improved performance of thin film solar cells based on Cu(In, Ga)S$_2$, Thin Solid Films **415**, 266 (2002).

[6] S. Merdes, D. Abou-Ras, R. Mainz, R. Klenk, M. Ch. Lux-Steiner, A. Meeder, H. W. Schock, and J. Klaer, CdS/Cu(In, Ga)S$_2$ based solar cells with efficiencies reaching 12.9% prepared by a rapid thermal process, Prog. Photovoltaics: Res. Appl. **21**, 88 (2013).

[7] T. Unold, I. Sieber, and K. Ellmer, Efficient CuInS$_2$ solar cells by reactive magnetron sputtering, Appl. Phys. Lett. **88**, 213502 (2006).

[8] H. Hiroi, Y. Iwata, K. Horiguchi, and H. Sugimoto, 960-mV open-circuit voltage chacopyrite solar cells, IEEE J. Photovoltaics **6**, 309 (2016).

[9] H. Hiroi, Y. Iwata, S. Adachi, H. Sugimoto, and A. Yamada, New world-record efficiency for pure-sulfide Cu(In, Ga)S$_2$ thin-film solar cell with Cd-free buffer layer via KCN-free process, IEEE J. Photovoltaics **6**, 760 (2016).

[10] H. Hiroi, Y. Iwata, H. Sugimoto, and A. Yamada, Progress toward 1000-mV open-circuit voltage on chalcopyrite solar cells, IEEE J. Photovoltaics **6**, 1630 (2016).

[11] H. Sugimoto, H. Hiroi, Y. Iwata, and A. Yamada, presented at 27th PVSEC Japan (November, 2017).

[12] http://www.solar-frontier.com/eng/news/2019/0117_press.html

[13] M. A. Green, Y. Hishikawa, W. Warta, E. D. Dunlop, D. H. Levi, J. H-Ebinger, and A. W. H. Ho-Baillie, Solar cell efficiency tables (version 50), Prog. Photovoltaics: Res. Appl. **25**, 668 (2017).

[14] Y. Hashimoto, K. Takeuchi, and K. Ito, Band alignment at CdS/CuInS$_2$ heterojunction, Appl. Phys. Lett. **67**, 980 (1995).

[15] L. Weinhardt, O. Fuchus, D. Groß, G. Storch, E. Umbach, N. G. Dhere, A. A. Kadam, S. S. Kulkarni, and C. Heske, Band alignment at CdS/Cu(In, Ga)S$_2$ interface in thin-film solar cells, Appl. Phys. Lett. **86**, 062109 (2005).

[16] A. Ennaoui, M. Bar, J. Klaer, T. Kropp, R. Saez-Araoz, and M. Ch. Lux-Steiner, Highly-efficient Cd-free CuInS$_2$ thin-film solar cells and mini-modules with Zn(S, O) buffer layers prepared by an alternative chemical bath process, Prog. Photovolt.: Res. Appl. **14**, 499 (2006).

[17] S. Merdes, R. Saez-Araoz, A. Ennaoui, J. Klaer, M. Ch. Lux-Steiner, and R. Klenk, Recombination mechanisms in highly efficient thin film Zn(S, O)/Cu(In, Ga)S$_2$ based solar cells, Appl. Phys. Lett. **95**, 213502 (2009).

[18] P. Wurfel, The chemical potential of radiation, J. Phys. C: Solid State Phys. **15**, 3967 (1982).

[19] T. Unold and L. Gütay, Photoluminescence analysis of thin-film solar cells, in *Advanced Characterization Techniques for Thin Film Solar Cells* (Wiley-VCH, 2011), Chap 7, pp. 151–175.

[20] A. Neisser, I. Hengel, R. Klenk, Th. W. Matthes, J. Alvarez-Garcıa, A. Pérez-Rodriguez, A. Romano-Rodriguez, and M-Ch. Lux-Steiner, Effect of Ga incorporation in sequentially prepared CuInS$_2$ thin film absorbers, Sol. Energy Mater. Sol. Cells **67**, 97 (2001).

[21] F. Babbe, L. Choubrac, and S. Siebentritt, Quasi Fermi level splitting of Cu-rich and Cu-poor Cu(In, Ga)Se$_2$ absorbers layers, Appl. Phys. Lett. **109**, 082105 (2016).

[22] G. Rey, C. Spindler, F. Babbe, W. Rachad, M. Nuys, R. Carius, S. Li, C. Platzer-Björkman, and S. Siebentritt, Absorption Coefficient of a Semiconductor Thin Film From Photoluminescence, Phys. Rev. Appl. **9**, 064008 (2018).

[23] S. Fiechter, Y. Tomm, M. Kanis, R. Scheer, and W. Kautek, On the homogeneity region, growth modes and optoelectronic properties of chalcopyrite-type CuInS$_2$, Phys. Status Solidi B **245**, 1761 (2008).

[24] T. Walter, D. Braunger, H. Dittrich, Ch. Koble, R. Herberholz, and H. W. Schock, Sequential processes for the deposition of polycrystalline Cu(In, Ga)(S, Se)$_2$ thin films: Growth mechanism and devices, Sol. Energy Mater. Sol. Cells **41**, 355 (1996).

[25] D. Regesch, L. Gütay, J. K. Larsen, V. Deprédurand, D. Tanaka, Y. Aida, and S. Siebentritt, Degradation and Passivation of CuInSe$_2$, Appl. Phys. Lett. **101**, 112108 (2012).

[26] J. Binsma, L. Giling, and J. Bloem, Luminescence of CuInS$_2$, J. Lumin. **27**, 35 (1982).

[27] J. Eberhardt, K. Schulz, H. Metzner, J. Cieslak, Th. Hahn, U. Reislohner, M. Gossla, F. Hudert, R. Goldhahn, and W. Witthuhn, Epitaxial and polycrystalline CuInS$_2$ thin films: A comparison of opto-electronic properties, Thin Solid Films **515**, 6147 (2007).

[28] S. Siebentritt, L. Gütay, D. Regesch, Y. Aida, and V. Deprédurand, Why do we make Cu(In, Ga)Se$_2$ solar cells non-stoichiometric?, Sol. Energy Mater. Sol. Cells **119**, 18 (2013).

[29] D. Braunger, Th. Durr, D. Hariskos, Ch. Koble, Th. Walter, N. Wieser, and H. W. Schock, in Photovoltaic Specialists Conference (1996).

[30] M. Turcu, O. Pakma, and U. Rau, Interdependence of absorbers composition and recombination in Cu(In, Ga)(Se, S)$_2$ heterojunctions solar cells, Appl. Phys. Lett. **80**, 2598 (2002).

[31] See Supplemental Material at http://link.aps.org/supplemental/10.1103/PhysRevApplied.11.054052 for a comparison of: SEM cross sections of absorber layers grown at high temperatures; XRD patterns of the Cu-rich one-stage samples grown at different temperatures; room-temperature PL spectra of the samples deposited at high T_{dep}; EDX images showing cadmium distribution for one-stage Cu-rich and Cu-poor samples.